Receiving Polarisation Agile Active Antenna Based on Injection Locked Harmonic Self Oscillating Mixers

Carlos Vázquez, Samuel Ver Hoeye *Member, IEEE,*, Miguel Fernández, Germán León, Luis Fernando Herrán, and Fernando Las Heras *Senior Member*

***Abstract*—In this work, a polarisation agile active antenna with phase shifter elements based on Injection Locked Third Harmonic Self Oscillating Mixers is presented. This phase shifting topology provides the double functionality of continuous range phase shifter and downconverter. The phase shift value introduced by each circuit can be easily tuned through a DC voltage within a theoretical continuous range of 450°. The behaviour of the isolated phase shifter circuit is studied, both as a function of the control voltage and versus frequency, through harmonic balance and envelope transient simulations. The polarisation tuning performance of the complete active antenna is simulated, analysing the impact of the operating parameters of the phase shifter on the overall behaviour. A receiving polarisation agile antenna with an input frequency band centred at 11.25 GHz and an output frequency band centred at 1.5 GHz has been manufactured for the experimental validation of the simulated results. A continuous range of polarisation tuning has been observed, including two orthogonal linear polarisations along with left hand and right hand circular polarisation.**

***Index Terms*—polarization, receiving antennas, microstrip antennas, microwave phase shifters, injection locked oscillators.**

I. Introduction

RECONFIGURABLE antenna implementations have become widespread in recent years, owing to their capability to dynamically adjust some of their properties to the requirements of each particular scenario. In this context, polarisation agility is an interesting feature for an antenna, since it simplifies the implementation of frequency reuse techniques, which can nearly double the channel capacity, and allows a good polarisation matching between transmitter and receiver. Furthermore, as polarisation diversity has proven to be as effective as spatial diversity to mitigate the detrimental multipath fading, both in indoor [1] and outdoor [2], [3] environments, polarisation agile antenna topologies provide substantial implementation size and cost reductions.

Several works on polarisation agile antennas have been presented in the bibliography. Some passive topologies enable the selection of a discrete number of polarisation states by altering the antenna layout through solid state [4], [5], or piezoelectric [6] switches. Others implement a continuous range of polarisation tuning by attaching varactor loads to the radiating patch [7].

Most of the active topologies available in the literature rely on feeding two orthogonal linearly polarised radiating modes of the antenna with the same original signal, conveniently modified through phase shifting circuitry, in order to provide the polarisation tuning capability. Phase shifting solutions based on a single oscillator circuit injection locked at the first harmonic component of the oscillation, enable a theoretical phase shift range limited to 180° [8]. This phase shift range can be doubled by feeding each of the radiating modes with an independent oscillator, providing any kind of coupling between the circuits is avoided [9]. Mutually coupled topologies maintain the same 180° theoretical phase shift range, which can be doubled, as in [10], by extracting the second harmonic component of the oscillation. These theoretical ranges are generally reduced in the presence of noise to about 15% smaller experimentally observable phase shift ranges. Moreover, due to the appearance of noise precursors when operating close to the limits of the synchronisation range [11], the usable phase-shift range is generally further reduced to approximately 70% of the theoretical range.

Manuscript received April 19, 2005; revised January 11, 2007. This work was supported by the "Ministerio de Ciencia e Innovación" of Spain and "FEDER", under projects TEC2006-12254-C02-01/TCM, TEC2008-01638/TEC (INVEMTA) and CONSOLIDER-INGENIO CSD2008-00068 (TERASENSE), by the "Gobierno del Principado de Asturias" under the "Plan de Ciencia y Tecnología (PCTI)"/"FEDER-FSE" by the grants BP07-047, BP08-082, the projects EQP06-015, FC-08-EQUIP-06 and PEST08-02, and by the "Cátedra Telefónica" Universidad de Oviedo and "Fundación CTIC".

The authors are with the Department of Electrical Engineering, Universidad de Oviedo. Edificio Polivalente de Viesques, Módulo 8, planta 1, Campus de Viesques, E-33203, Gijón, Spain. e-mail: cvazquez@tsc.uniovi.es

With regard to receiving topologies, the phase shifting functionality can be attained through a mixing operation between the conveniently phase shifted self oscillation signal, (or one of its harmonic components), and the input signal. The architecture used in this work is based on an Injection Locked 3^{rd} Harmonic Self Oscillating Mixer (IL3HSOM) [12], in which the output signal is generated through mixing the input signal at frequency f_{in}, with the third harmonic component at frequency $3f_0$ of the HSOM self oscillation fundamental frequency f_0. As a result of this operation, a downconverted signal at $f_{IF} = f_{in} - 3f_0$ is obtained in a single stage [12], with the desired phase shift within a theoretical range of 540° (which assures a usable range of at least 360°).

In this paper, a receiving polarisation agile microstrip antenna is presented. The wide phase shift range provided by the IL3HSOM based phase shifters, enable the antenna polarisation tuning within a continuous range, comprising two orthogonal linear polarisations and both left hand and right hand circular polarisation (LHCP and RHCP). Additionally, another two linear polarisations might be produced by activating only one circuit at a time. However, these are not considered in this work since the received power would be halved, as it would be with any other of the available polarisations.

The paper is structured as follows. In Section II, the proposed topology is introduced and the individual performance of its important parts is studied. In Section III, the polarisation tuning capabilities of the complete active antenna solution are simulated (using Advanced Design System), for different operating conditions of the phase shifter circuits. In Section IV, the experimental results obtained with the manufactured receiving polarisation agile antenna are shown.

II. Polarisation Agile Antenna Based on IL3HSOM

A. Topology of the Polarisation Agile Antenna

The topology of the receiving polarisation agile antenna is shown in Fig. 1(a). A two port Aperture Coupled Patch Antenna (ACPA), couples the power received in each of its two orthogonal linearly polarised fundamental modes, at $f_{in} = 11.15 - 11.35$ GHz, onto one of its output ports, which deliver these signals to two IL3HSOM based phase shifters. Both IL3HSOM circuits are injection locked to an external signal of power P_s, frequency $f_s = 3.25$ GHz and phase ϕ_s, through a Wilkinson power divider, providing equal power and phase in both branches ($P_{s_1} = P_{s_2}$ and $\phi_{s_1} = \phi_{s_2}$).

Using the techniques presented in [13]–[15], the IL3HSOM circuits have been optimised to provide maximum conversion gain ($G_{c_i} = P_{IF_i}/P_{in_i}, \quad i \in \{1, 2\}$) in the input frequency band at $f_{in} = 11.15 - 11.35$ GHz, for the mixing operation $f_{IF} = f_{in} - 3f_0$. The phase shifts introduced by the IL3HSOM circuits at intermediate frequency, with respect to the external phase reference ($\Delta\phi_i = \phi_{IF_i} - \phi_s$, $i \in \{1, 2\}$), can be separately controlled through two DC signals, enabling the polarisation tuning capability. Low power samples of the output signals of both circuits are extracted through microstrip directional couplers for phase shift monitoring purposes. The sampled signals are simultaneously measured with two Agilent 89600 Vector Signal Analysers (N8201A - N8221A). The output signal of the polarisation agile antenna is obtained through a Wilkinson combiner and measured with the vector network analyser of the anechoic chamber measurement setup, which is explained in Section IV.

In order to prevent detrimental reductions in the phase shift ranges of the IL3HSOM circuits and to assure their independent performance, mutual coupling between them at the harmonic components of the self oscillation frequency, (Nf_0, $N = 1, \ldots, 8$), must be avoided. The required isolation levels through the input and output

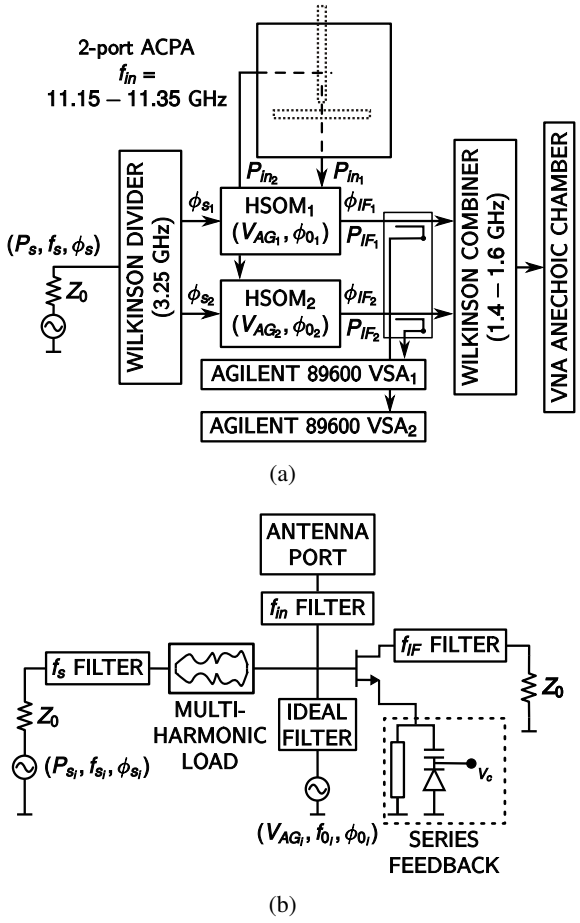

Fig. 1. (a) Topology of the polarisation agile antenna. (b) Circuit diagram of the IL3HSOM based phase shifter.

ports are achieved by filtering, taking advantage of the fact that none of these harmonic components falls into either the input or output frequency bands. Mutual coupling through the synchronisation port at the harmonic components (Nf_0, $N = 2, \ldots, 8$) is avoided by the bandpass filter centred at $f_s = f_0$. The Wilkinson divider is designed to feature high isolation levels, so that the synchronisation signal for both circuits is exclusively determined by the external generator.

B. Two Port Aperture Coupled Patch Antenna

The antenna, as depicted in Fig. 2(a), consists of a square patch designed in the bottom layer of a 0.762 mm thick ARLON 25N substrate ($\epsilon_r = 3.38$ and $\tan\delta = 0.0025$ at 10 GHz) and placed inverted on top of a 2.6 mm thick foam layer ($\epsilon_r = 1.07$ and $\tan\delta = 0.0041$ at 10 GHz). The power received in each of the two orthogonal linearly polarised fundamental modes of the patch is electromagnetically coupled through two perpendicular slots etched in the ground plane of the distribution network, onto the microstrip transmission line connected to one of the output ports. These transmission lines are designed to have a 90 degree difference in electrical length, in order for the output signals to be in phase when the incident radiation presents right hand circular polarisation.

A prototype of the antenna has been manufactured and measured. An impedance matched frequency band ($S_{ii} < -10$ dB, $i \in \{1, 2\}$) from 10.5 to 12 GHz is obtained, as shown in Fig. 2(b). High isolation levels between the ports ($S_{12} < -30$ dB), are observed throughout the same band.

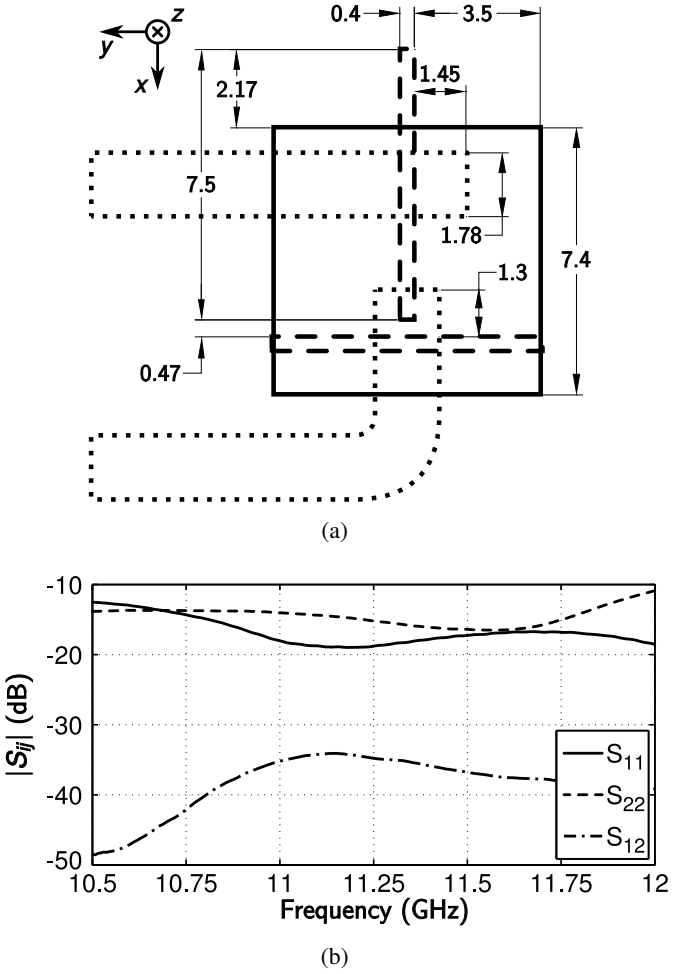

Fig. 2. (a) Structure of the two port aperture coupled patch antenna. Dimensions in millimetres. (b) Measured scattering parameters of the two port ACPA.

C. Performance of the IL3HSOM based phase shifters

The circuit topology of the IL3HSOM is shown in Fig. 1(b). The series feedback at the source terminal of the ATF36077 transistor is designed to produce negative resistance at the gate port. The component at intermediate frequency resulting from the mixing operation is selected through a bandpass filter at the drain port and, as a reference for the phase shifting functionality, a signal of frequency f_s and power P_s is injected through the synchronisation filter at the gate port. A varactor diode connected to the series feedback network provides the phase shift tuning capability.

For different operation conditions, the injection locked solutions of the IL3HSOM circuit are obtained using the techniques presented in [12], based on the use of an auxiliary generator in harmonic balance and envelope transient simulations. At the centre frequency of the input band $f_{in_c} = 11.25$ GHz, the synchronised solutions for both the conversion gain G_c, and the phase shift introduced by the circuit at intermediate frequency, with respect to the external phase reference $\Delta\phi = \phi_{IF} - \phi_s$, have been calculated as a function of the control voltage V_c. The results for three different synchronisation power levels are shown in Fig. 3. The traces in dashed line correspond to harmonic balance simulations and represent mathematical solutions of the system. However, only a limited range of these solutions are stable and thus, experimentally observable [12]. For values of the control voltage outside the stable ranges, which are determined using envelope transient simulations and indicated in solid line, the frequency of oscillation is no longer locked to that of the synchronisation signal and it starts to vary with the control voltage.

The conversion gain is slightly dependent on the control voltage (Fig. 3(a)) and, although this dependence increases with the synchronisation power P_s, it is not significant for most applications since, in the worst case ($P_s = -30$ dBm), its variation range remains below 0.7

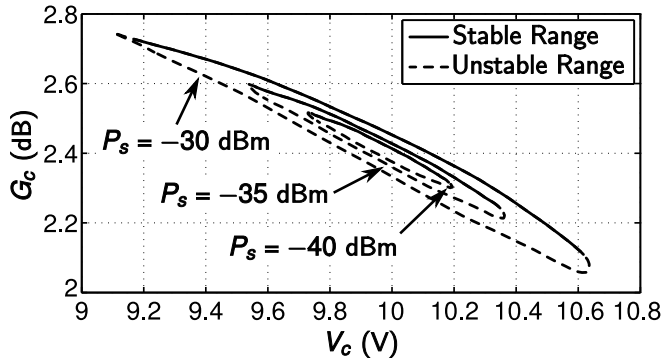

(a)

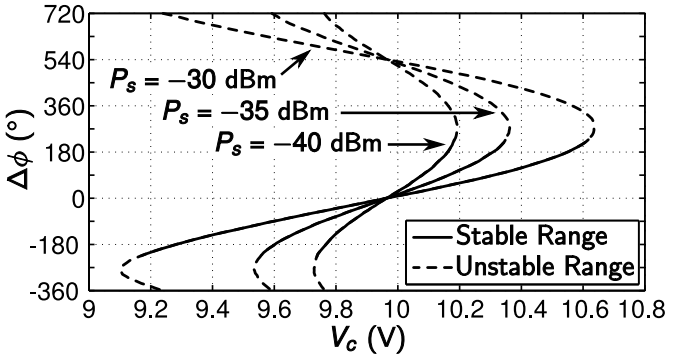

(b)

Fig. 3. Injection locked solutions of the isolated IL3HSOM circuit for three different synchronisation power levels P_s, as a function of the control voltage V_c, for (a) the conversion gain G_c, and (b) the phase shift at intermediate frequency $\Delta\phi$. The stable and unstable regions determined through envelope transient simulations [12], are also indicated.

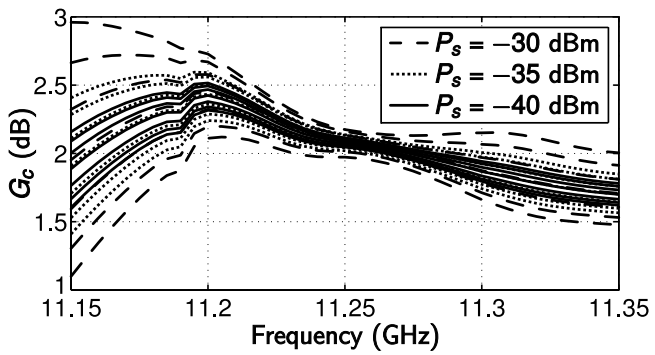

(a)

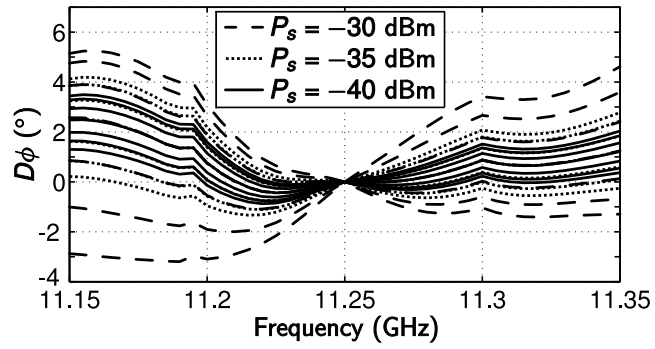

(b)

Fig. 4. Frequency response of the IL3HSOM circuit for three different synchronisation power levels and for seven working points, uniformly distributed throughout the stable ranges (a) Conversion gain. (b) Phase deviation $D\phi$, as defined in (1).

dB. By tuning the varactor control voltage V_c, the phase shift $\Delta\phi$ can be controlled within a stable range of about 450 degrees (Fig. 3(b)). Even though the sensitivity to the control signal is higher for lower synchronisation power levels, the stable range of variation is approximately the same for the three studied cases.

Hence, the phase shift introduced at the centre frequency $\Delta\phi(f_{in_c})$, can be arbitrarily selected within the synchronisation ranges through the varactor bias voltage. However, once $\Delta\phi(f_{in_c})$ is fixed at a specific point, the phase shifts introduced at other frequencies cannot be controlled, as they are determined by the frequency response of the circuit. For three synchronisation power levels, this frequency response has been calculated through harmonic balance and envelope transient simulations, considering seven different phase shift values set at the centre frequency $\Delta\phi(f_{in_c})$, uniformly distributed throughout the corresponding stable ranges (Fig. 3(b)).

The frequency response of the conversion gain G_c, is represented in Fig. 4(a). For higher synchronisation power levels, a stronger variation is observed, both with frequency and with the operation point selected ($\Delta\phi(f_{in_c})$), especially when approaching the limits of the input frequency band. In order to simplify the comparison between the multiple traces represented, the phase deviation $D\phi$ has been defined in (1). The first term of the equation is the actual frequency response of the circuit, for the different control voltages V_c considered. By subtracting the second term (the phase shift value established at the centre frequency $\Delta\phi(f_{in_c}, V_c, P_s)$, for each different trace), the offset between traces is eliminated, putting them together at the centre frequency.

$$D\phi(f, V_c, P_s) = \Delta\phi(f, V_c, P_s) - \Delta\phi(f_{in_c}, V_c, P_s) - L(f, P_s) + L(f_{in_c}, P_s) \quad (1)$$

Due to the propagation throughout the circuit, the phase response presents the characteristic strong slope as a function of frequency which, in this case, conceals the small differences between the traces. Thus, for each of the considered synchronisation power levels, the linear least squares fitting of the trace corresponding to the centre of the stable phase shift range (Fig. 3(b)), $L(f, P_s)$, is calculated to cancel out this slope. The last term of

(1) sets the deviation to zero at the centre frequency ($D\phi(f_{in_c}, V_s, P_s) = 0$).

As shown in Fig. 4(b), the phase deviation $D\phi$ also increases its variation, both with frequency and with the operation point selected ($\Delta\phi(f_{in_c})$), for higher synchronisation power levels. The impact of the frequency performance of the circuit on the present application is studied in the next section.

III. Polarisation Tuning Performance of the Active Antenna

The polarisation tuning capability is attained by introducing a relative phase shift between the signals present at the output ports of the antenna. According to the antenna layout outlined in Fig. 2(a), the component corresponding to the fundamental mode polarised along the x axis, V_x, undergoes a 90 degree phase delay with respect to the other, V_y, in order to obtain circular polarisation when both components are combined in phase. The theoretical evolution of the antenna polarisation when an additional phase shift α is introduced in the V_x component ($V_{out} = g_x V_x e^{j(\alpha-90)} + g_y V_y$), is shown in Fig. 5 in terms of its Axial Ratio (AR), as expressed in (2), assuming both components are combined with equal voltage gain ($g_x = g_y = 1$).

$$AR = \cot\left|\frac{1}{2}\arcsin\left(\frac{2g_x g_y}{g_x^2 + g_y^2}\sin(\alpha - 90)\right)\right| \qquad (2)$$

The Axial Ratio is defined as the relationship between the major and the minor axes of the polarisation ellipse of the plane wave propagating along the $+z$ direction, that results in maximum available power at the antenna global output [16].

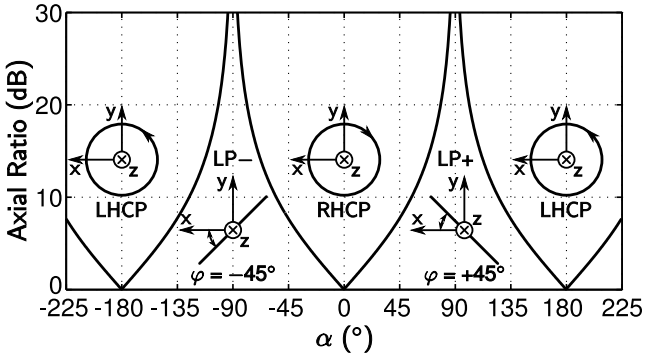

Fig. 5. Theoretical evolution of the antenna polarisation when a phase shift α is introduced in the V_x component (in addition to the 90 degree delay caused by the feeding network layout).

When both components are combined in phase ($\alpha = 0°$), the axial ratio drops to zero, corresponding to right hand circular polarisation (RHCP). The axial ratio is likewise zero for $\alpha = \pm 180°$, obtaining left hand circular polarisation (LHCP). For $\alpha = 90°$ and $\alpha = -90°$, two linear polarisations ($AR > 30$ dB) are achieved in the $\varphi = +45°$ and $\varphi = -45°$ directions respectively (hereafter referred to as LP+ and LP−).

The behaviour of the complete active antenna topology, as shown in Fig. 1(a), has been simulated for three different values of the synchronisation power P_s. The control voltage of HSOM$_1$, V_{c_1}, has been swept throughout its stable range (Fig. 3(b)), while keeping HSOM$_2$ working at the centre point, which replicates the theoretical case studied above. In Fig. 6(a), the evolution of the axial ratio as a function of the control voltage V_{c_1}, has been represented. As the phase shift $\Delta\phi$ produced by the IL3HSOM circuits is a monotonically increasing function of the control voltage (Fig. 3(b)), the peaks and minima in this case represent the same polarisation states indicated in Fig. 5. For each of the synchronisation power levels considered, the performance at six frequency points, uniformly distributed throughout the input band ($f_k = 11.11 + 0.04k$ GHz, $k = 1, \ldots, 6$), have been displayed.

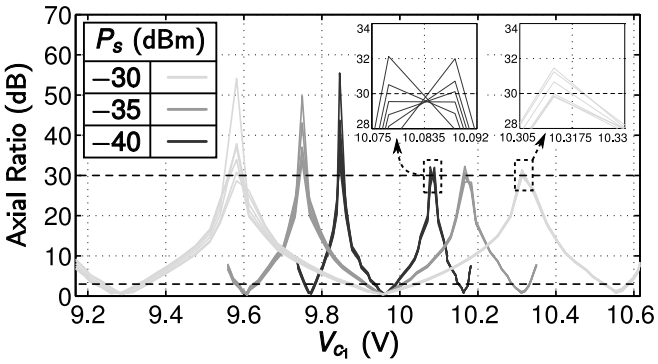

(a)

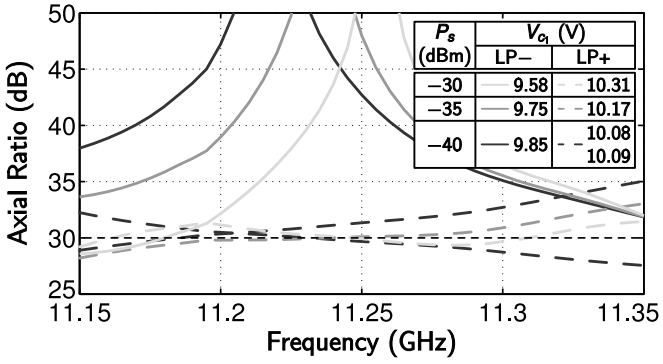

(b)

Fig. 6. (a) Variation of the axial ratio at the centre of the input frequency band ($f_{in_c} = 11.25$ GHz), as the control voltage V_{c_1} is swept, while keeping HSOM$_2$ working at the centre point. For each synchronisation power level, the behaviour at six points of the input frequency band is displayed. (b) Variation of the axial ratio over frequency for the working points specified in the legend.

Both circular polarisations are successfully obtained ($AR < 3$ dB), for all the synchronisation power levels and at all the frequency points considered. With linear polarisations, on the other hand, due to their higher sensitivity to the phase shift (Fig. 5), a somewhat more frequency selective response is observed. This is especially apparent for $P_s = -30$ dBm, where both linear polarisations ($AR > 30$ dB) are only achieved at some frequencies. For the two lower synchronisation power levels ($P_s = -35$ and $P_s = -40$ dBm), LP$-$ is stable for all the considered frequency values, whereas for LP+, the axial ratio drops below the 30 dB threshold at some point. The behaviour for $P_s = -40$ dBm has been magnified in the first inset of Fig. 6(a), showing peaks at two successive V_{c_1} values, which take place at different frequency points (Fig. 6(b)). This suggests the existence of an intermediate working point between those two, providing higher axial ratio levels, together with a better frequency performance.

The variation of the axial ratio over frequency is shown in Fig. 6(b). Since the circular polarisations have been found to be stable in the input band (Fig. 6(a)), only the linear ones, corresponding to the working points specified in the legend, have been represented. For $P_s = -40$ dBm, the behaviour at the two successive V_{c_1} values corresponding to LP+ have been included, showing linear polarisation in two different frequency ranges. The most limited frequency performance is observed for $P_s = -30$ dBm. The polarisation LP$-$ is maintained along the input band for the two lower synchronisation power levels, whereas for LP+, the axial ratio drops below 30 dB at some point within this band.

In conclusion, the performance of the IL3HSOM based phase shifter circuit is more stable over frequency for lower values of the synchronisation power, as discussed in Section II-C, leading to potentially wider polarisation bandwidths. Nevertheless, since the phase shift can be varied within a continuous range, the working point selected also has an important impact on the frequency performance, especially for linear polarisations.

IV. Experimental Results

In order to validate the simulated results, the proposed polarisation agile active antenna has been manufactured and assembled following the topology of Fig. 1(a). Due to the fact that the signal received by the antenna is internally downconverted, obtaining its output at intermediate frequency, the anechoic chamber measurement setup shown in Fig. 7, was needed to evaluate the global performance of the system (polarisation tuning capabilities, radiation patterns, ...).

A horn antenna with high polarisation purity, fed by an external Signal Generator (SG), is used to transmit a tone in the input frequency band $f_{in} = 11.15 - 11.35$ GHz. Another external signal generator provides the synchronisation signal at frequency f_s to the active antenna, which is mounted on the azimuthal positioner. The output of the system at intermediate frequency is measured by a vector network analyser, which is triggered by the positioning control system. The sampled IF output of each IL3HSOM circuit is separately monitored by an Agilent 89600 Vector Signal Analyser (N8201A - N8221A). All the measurement and signal generation equipment is synchronised through a 10 MHz pilot signal, which provides a common frequency reference.

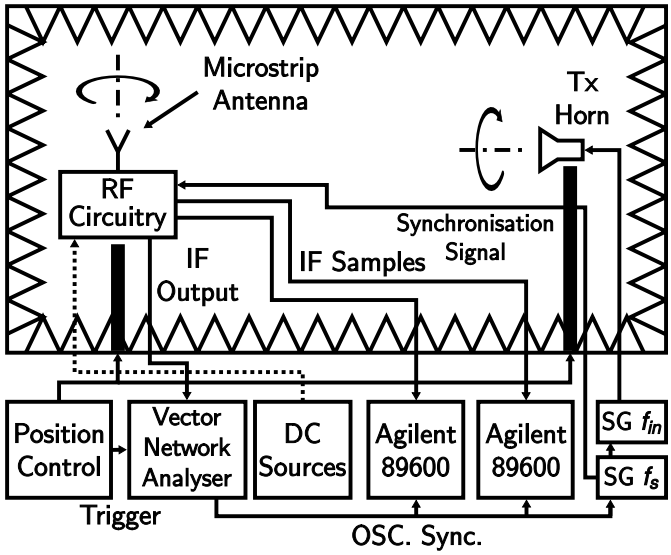

Fig. 7. Measurement setup in the anechoic chamber.

The polarisation state of the active antenna is evaluated by registering the relative power received at the IF output, while the transmitting horn is rotated about its longitudinal axis. This procedure is repeated for different operation points as the control voltage V_{c_1} is swept throughout the synchronisation range. Since simulations showed a better performance for lower values of the synchronisation power, these measurements have been carried out for $P_s = -35$ and $P_s = -40$ dBm. For the centre frequency of the input band ($f_{in_c} = 11.25$ GHz), the relative IF power measured at the output of the active antenna is shown in Fig. 8, as a function of the control voltage V_{c_1} and the polarisation angle of the transmitting horn. For the sake of clarity, only a representative group of the measurements carried out has been represented in this figure.

The axial ratio, measured at the centre frequency of the input band, as a function of the control voltage is shown in Fig. 9(a) for $P_s = -35$ and $P_s = -40$ dBm.

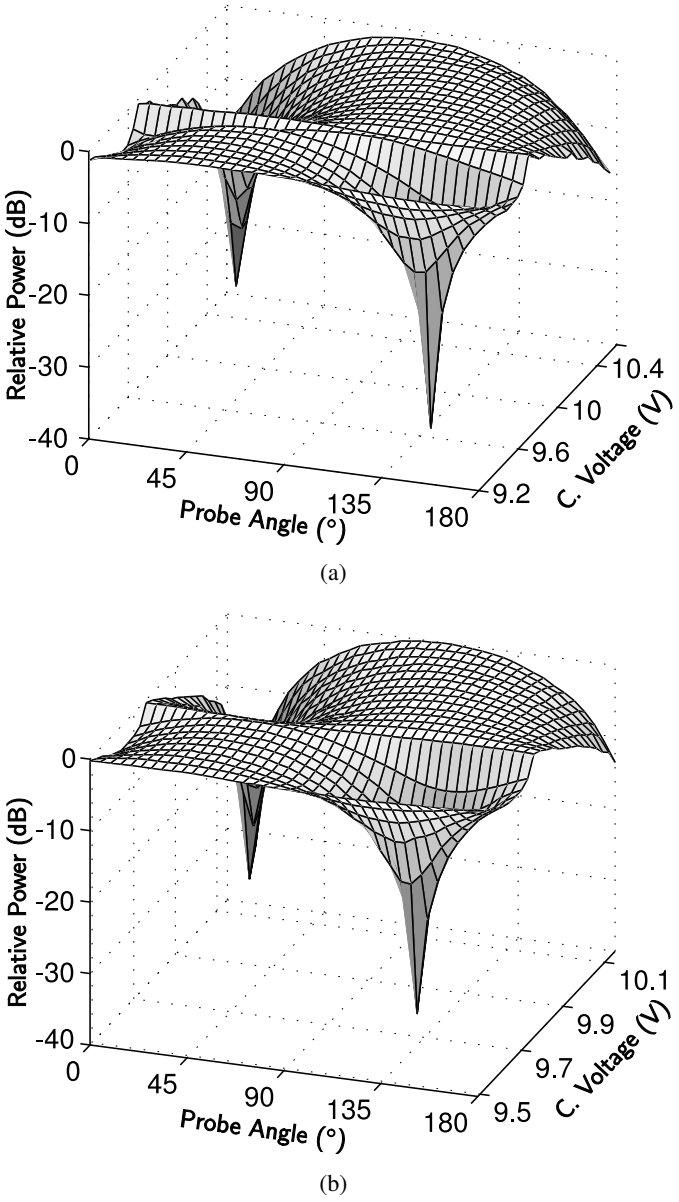

Fig. 8. Relative IF power measured at the output of the active antenna at the centre frequency of the input band ($f_{in_c} = 11.25$ GHz), as a function of the control voltage and the polarisation angle of the probe for: (a) $P_s = -35$ dBm. (b) $P_s = -40$ dBm.

A small deviation on the performance of the manufactured HSOM circuits has been found, producing stronger variations of the conversion gain with the control voltage, especially at the upper end of the synchronisation range. Although, as a consequence of this deviation, the second left hand circular polarisation observed in simulation (corresponding to the higher value of the control signal), is not reached in measurement, all the desired polarisations have been successfully attained. Furthermore, note that, for this experimental setup the second HSOM circuit has been kept at a fixed working point and therefore, a double phase shift tuning range is available.

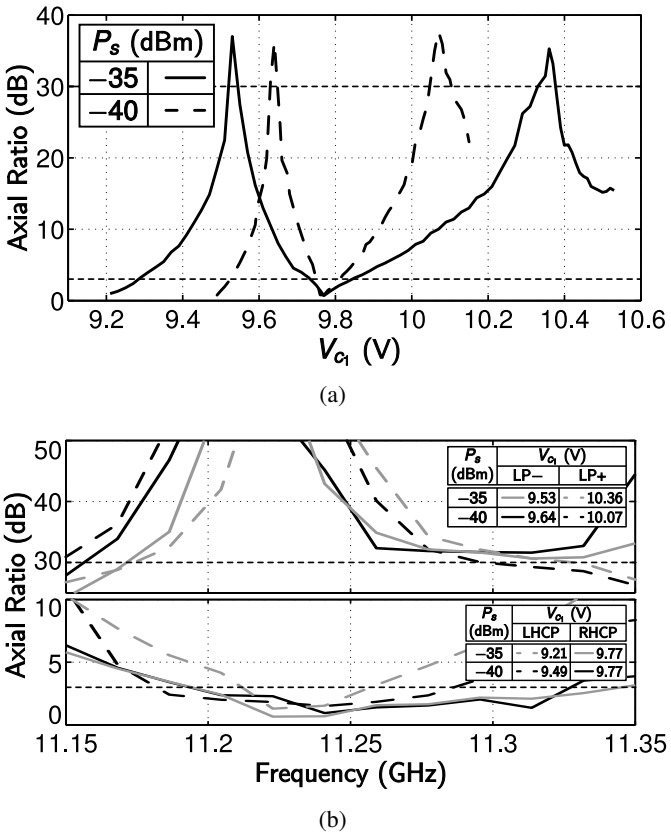

Fig. 9. Measurement of the axial ratio for $P_s = -35$ and $P_s = -40$ dBm. (a) As a function of the control voltage V_{c_1} at the centre of the input frequency band ($f_{in_c} = 11.25$ GHz). (b) As a function of frequency for LP− and LP+ (upper subfigure), and for RHCP and LHCP (lower subfigure).

The variation of the axial ratio over frequency is represented in Fig. 9(b) for the two orthogonal linear polarisations (LP+ and LP−), and for RHCP and LHCP. Unlike in the simulation, the values of the control signal V_{c_1} have been carefully selected to produce the best possible frequency performance. Both linear polarisations are maintained over almost the whole input frequency band for both synchronisation values, although a slightly wider bandwidth is observed for $P_s = -40$ dBm.

The stronger variation in the conversion gain of the practical circuits mentioned earlier, has a greater impact on the circular polarisations, which present a poorer frequency performance. The polarisation bandwidth is reduced with respect to the simulated results, although for $P_s = -40$ dBm, the axial ratio remains below the 3 dB threshold throughout a substantial part of the band.

The radiation pattern of the active antenna at $f_{in_c} = 11.25$ GHz, has been measured by rotating it about the azimuthal angle θ, while the polarisation of the transmitting horn is oriented in the $\varphi = 45°$ direction.

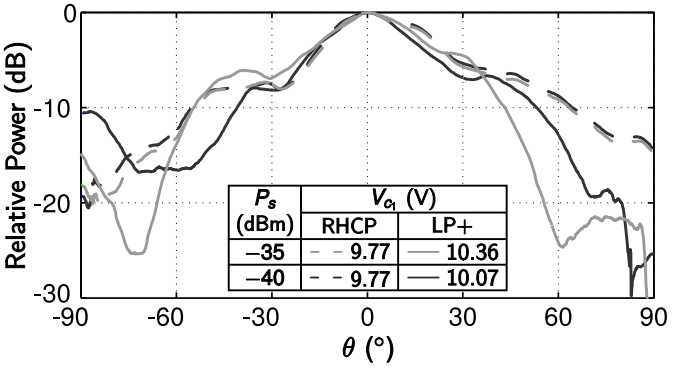

Fig. 10. Radiation pattern of the active antenna at $f_{in_c} = 11.25$ GHz, for LP+ and RHCP and for two synchronisation power levels, measured with the polarisation of the transmitting oriented in the $\varphi = 45^\circ$ direction.

The results are displayed in Fig. 10 for two different synchronisation power levels.

V. Conclusion

A receiving polarisation agile active antenna based on injection locked third harmonic self oscillating mixers has been presented. The multifunctional IL3HSOM circuits have proven to be an interesting phase shifting solution, providing efficient integrated signal downconversion, which enables the implementation of compact, low cost and low power consuming receiving systems. The proposed topology enables the polarisation variation in a continuous range, comprising two orthogonal linear polarisations along with left hand and right hand circular polarisation. The frequency performance of the complete system has been studied, observing a better behaviour for lower synchronisation power levels. The simulated results have been validated by measurements of the manufactured prototype, obtaining a good agreement.

References

[1] S. Loredo, B. Manteca, and R. Torres, "Polarization diversity in indoor scenarios: an experimental study at 1.8 and 2.5 ghz," *Personal, Indoor and Mobile Radio Communications, 2002. The 13th IEEE International Symposium on*, vol. 2, pp. 896–900 vol.2, Sept. 2002.

[2] A. Turkmani, A. Arowojolu, P. Jefford, and C. Kellett, "An experimental evaluation of the performance of two-branch space and polarization diversity schemes at 1800 mhz," *Vehicular Technology, IEEE Transactions on*, vol. 44, no. 2, pp. 318–326, May 1995.

[3] F. Lotse, J.-E. Berg, U. Forssen, and P. Idahl, "Base station polarization diversity reception in macrocellular systems at 1800 mhz," *Vehicular Technology Conference, 1996. 'Mobile Technology for the Human Race'., IEEE 46th*, vol. 3, pp. 1643–1646 vol.3, Apr-1 May 1996.

[4] R.-H. Chen and J.-S. Row, "Single-fed microstrip patch antenna with switchable polarization," *Antennas and Propagation, IEEE Transactions on*, vol. 56, no. 4, pp. 922–926, April 2008.

[5] Y. Sung, T. Jang, and Y.-S. Kim, "A reconfigurable microstrip antenna for switchable polarization," *Microwave and Wireless Components Letters, IEEE*, vol. 14, no. 11, pp. 534–536, Nov. 2004.

[6] S.-H. Hsu and K. Chang, "A novel reconfigurable microstrip antenna with switchable circular polarization," *Antennas and Wireless Propagation Letters, IEEE*, vol. 6, pp. 160–162, 2007.

[7] P. Haskins and J. Dahele, "Varactor-diode loaded passive polarisation-agile patch antenna," *Electronics Letters*, vol. 30, no. 13, pp. 1074–1075, Jun 1994.

[8] P. Hall, I. Morrow, P. Haskins, and J. Dahele, "Phase control in injection locked microstrip active antennas," *Microwave Symposium Digest, 1994., IEEE MTT-S International*, pp. 1227–1230 vol.2, May 1994.

[9] C. Vázquez, S. Ver Hoeye, M. Fernández, L. Herrán, G. León, and F. Las Heras, "Transmitting polarisation agile antenna based on synchronised oscillators," in *Antennas and Propagation Society International Symposium, 2009. AP-S 2009. IEEE*, July 2009, pp. 1–4.

[10] S.-C. Yen and T.-H. Chu, "A beam-scanning and polarization-agile antenna array using mutually coupled oscillating doublers," *Antennas and Propagation, IEEE Transactions on*, vol. 53, no. 12, pp. 4051–4057, Dec. 2005.

[11] S. Ver Hoeye, A. Suárez, and S. Sancho, "Analysis of noise effects on the nonlinear dynamics of synchronized oscillators," *Microwave and Wireless Components Letters, IEEE*, vol. 11, no. 9, pp. 376–378, Sep 2001.

[12] S. Ver Hoeye, L. F. Herrán, M. Fernández, and F. Las Heras, "Design and analysis of a microwave large-range variable phase-shifter based on an injection-locked harmonic self-oscillating mixer," *IEEE Microw. Wireless Compon. Lett.*, vol. 16, no. 6, pp. 342–344, Jun. 2006.

[13] S. Ver Hoeye, L. Zurdo, and A. Suárez, "New nonlinear design tools for self-oscillating mixers," *IEEE Microw. Wireless Compon. Lett.*, vol. 11, no. 8, pp. 337–339, Aug. 2001.

[14] L. F. Herrán, S. Ver Hoeye, and F. Las Heras, "Nonlinear optimization tools for the design of microwave high-conversion gain harmonic self-oscillating mixers," *IEEE Microw. Wireless Compon. Lett.*, vol. 16, no. 1, pp. 16–18, Jan. 2006.

[15] M. Fernandez, S. Ver Hoeye, L. Herran, and F. Las Heras, "Nonlinear optimization of wide-band harmonic self-oscillating mixers," *Microwave and Wireless Components Letters, IEEE*, vol. 18, no. 5, pp. 347–349, May 2008.

[16] C. Balanis, *Antenna Theory, Analysis and Design*. Wiley, 1982.

Carlos Vázquez Antuña received the M.Sc. degree in telecommunication engineering from the University of Oviedo, Gijón, Spain, in 2007 and he is currently pursuing the Ph.D. degree.

Since 2007, he has been working as a Research Assistant with the Signal Theory and Communications Area, at the University of Oviedo. His research efforts mainly focus on nonlinear analysis and the optimisation of microwave circuits to be used in active antennas.

Samuel Ver Hoeye (M'05) received the M.Sc. degree in electronic engineering from the University of Gent, Gent, Belgium, in 1999, and the Ph.D. degree from the University of Cantabria, Santander, Spain, in 2002.

He is currently Associate Professor with the Department of Electrical and Electronic Engineering of the University of Oviedo, Gijón, Spain. His main research is focused on nonlinear analysis and the optimisation of microwave circuits and their application to active antennas.

Miguel Fernández García received the M. Sc. degree in telecommunication engineering from the University of Oviedo in 2006, and he is currently working towards the Ph.D. degree.

From 2005 to 2008, Mr. Fernández worked as a Research Assistant with the Signal Theory and Communications Area, at the University of Oviedo, where he is currently an Assistant Professor. His main interest are focused on nonlinear analysis and the optimisation of microwave circuits to be used in active and phased antenna arrays.

Germán León Fernández was born in Alcázar de San Juan, Spain, in 1975. He received the Bachelor's degree and the Ph. D. degree in Physical Science in 1998 and in 2005, both from the University of Seville, Spain. In 2005 he joined the Department of Electrical Engineering at University of Oviedo, Spain, as an Associate Professor. His research interests focus on antenna measurements, characterization and planar antennas design.

Luis Fernando Herrán Ontañón received the Telecommunication Engineering degree from the University of Cantabria, Santander, in 1999, and the Ph.D. degree from the University of Oviedo, Gijón, Spain, in 2007.

In 2003, he joined the Department of Electrical Engineering at the University of Oviedo. His research interest includes nonlinear optimisation of phased array antennas and the design of RF/microwave subsystems.

Fernando Las Heras Andrés (M'86-SM'08) received the M.S. degree in 1987 and the Ph.D. degree in 1990, both in telecommunication engineering, from the Universidad Politécnica de Madrid (UPM), Madrid, Spain.

From 1988 to 1990, he was a National Graduate Research Fellow. From 1991 to 2000, he was an Associate Professor with the Department of Signals, Systems and Radiocommunications, UPM. From 2001 to 2003, he was an Associate Professor with the Department of Electrical Engineering, University of Oviedo, Gijón, Spain, pioneering the Area of Theory of Signal and Communications. Since December 2003, he has been a Full Professor at the University of Oviedo. His main research interests include the analysis and design of antennas, electromagnetic interference (EMI), and the inverse electromagnetic problem with application to diagnostic, measurement and synthesis of antennas.